

Non-revisiting Coverage Task with Minimal Discontinuities for Non-redundant Manipulators

Abstract—A theoretically complete solution to the optimal Non-revisiting Coverage Path Planning (NCP) problem of any arbitrarily-shaped object with a non-redundant manipulator is proposed in this work. Given topological graphs of surface cells corresponding to feasible and continuous manipulator configurations, the scheme is aimed at ensuring optimality with respect to the number of surface discontinuities, and extends the existing provable solution attained for simply-connected configuration cell topologies to any arbitrary shape. This is typically classified through their genus, or the number of “holes” which appear increasingly as configurations are further constrained with the introduction of additional metrics for the task at hand, e.g. manipulability thresholds, clearance from obstacles, end-effector orientations, tooling force/torque magnitudes, etc.

The novel contribution of this paper is to show that no matter what the resulting topological shapes from such quality cell constraints may be, the graph is finitely solvable, and a multi-stage iterative solver is designed to find all such optimal solutions.

I. INTRODUCTION

Full coverage of the surface of a given object with non-redundant manipulators is embodied in tasks such as automatic polishing, deburring, painting or surface inspection, where the need for non-repetitive path planning is paramount to avoid over revisiting.

The kinematic relationship of a typical manipulator makes mapping between work- and joint-space non-bijective [12], which in effect drives coverage paths to be traditionally carried out in the former to ensure no revisiting of points in the surface [15]. However, in further pursuing motions where the manipulator may minimise the number of reconfigurations is obliged to undertake to follow a desirable continuous end-effector (EE) path, a global optimal cellular decomposition problem in joint-space has been proposed to incur joint-space partitions with minimum sets [20]. This is illustrated in the example shown by Fig. 1: the external surface of a wok-like object is inspected by a non-redundant manipulator. Points on the surface can be reached by a variety of robot configurations. The three solid colour cells shown in Fig. 1(b) illustrate poses of disjoint sets reachable as a continuous set by a given configuration, visually seen by the different colours. These cells become the elements on a topological graph Fig. 1(c), where each possible colour of a cell is recorded. A cellular decomposition splits and merges the cells to transform the process into that of painting all points in the graph with one of the possible colours, driven by attaining a minimum set which equates to least number of EE lift-offs. One such optimal solution with 2 lift-offs is illustrated in Fig. 1(d), whereby any arbitrary continuous path within a colour surface area

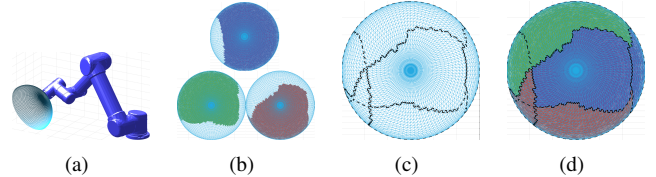


Fig. 1. Example of simply-connected cell coverage. (a) Hemispherical object placed in the workspace. (b) Simply-connected cells of three valid robot configurations, chosen by the optimal solution shown in (d). (c) Topological graph. (d) One optimal solution requiring 2 lift-offs.

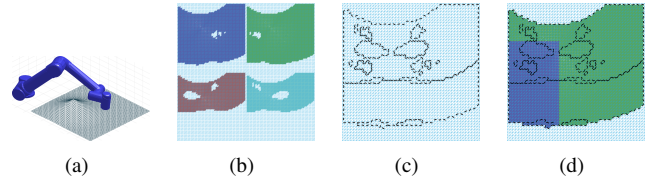


Fig. 2. Example of multiply-connected cell coverage. (a) Irregular “hilly” object placed in the workspace. (b) Multiply-connected cells of four valid robot configurations, chosen by the optimal solution shown in (d). (c) Topological graph. (d) One optimal solution requiring 1 lift-off.

will result in maximum joint continuity of the global path. The addition of obstacles and the relative pose of robot and object further condition the final solution. For further details please refer to [20].

A critical assumption however is that the constituent surface points necessarily adopt simply-connected space topologies. This is reasonable for simple shapes and sparse obstacle environments, but becomes unrealistic as objects grow in complexity, or with the imposition of increasing motion constraints, generically deriving in multiply-connected cells. An illustrative example is given in Fig. 2 where a manipulator moving over a “hilly” terrain generates reachable areas in the mesh which contains non simply-connected cells. This is further compounded when additional or more restrictive constraints are imposed, as will be seen later in the results when the degree of manipulability is also considered and more “cavities” appear in the configuration cells and generated topological graphs.

Since the shape of cells can be classified through their genus, i.e., the number of “holes” within the cell, in this work a theoretically complete solution is given by solving for cells with all possible genus. The key observation of the proposed algorithm is that whatever genus the cell is, the number of lift-off to cover it is always zero. A direct reflection from this is thus to reduce the genus of the cell gradually by cell divisions

to eventually make it equivalent to a simply-connected cell which has been proven finitely solvable. This however is non-trivial: the place to put a cutting path to transform a genus-one cell into a simply-connected cell directly effects the order of edges on the boundary of the sub-cells, leading to different structures. Existing algorithms in the literature are not able to provide a systematic cell decomposition solution to accomplish a guaranteed transformation from an initial graph containing large genus cells into simply connected topologies. This is provided in this work through the analysis of equivalent topological divisions. To that extent, the finiteness of all possible divisions is first proven for a genus-one cell as building block. A multi-stage iterative solver can then be introduced to transform higher-genus cells into lower-genus cells. The two novel contributions of this paper can be thus summarised as:

- 1) Providing the necessary conditions to be able to apply the surface modeling described by the proposed topological graph structure.
- 2) Proposing a systematic solution to be applicable for any genus- n cell topology.

The remainder of this paper ¹ is organised as follows. Section II reviews existing literature. Section IV proves the necessary conditions to apply the proposed algorithm. Section V briefly restates the existing results in [20] to solve for simply-connected cells. Section VI goes into further details about the finiteness of solving elementary genus-one cells, whilst a multi-stage iterative strategy to solve for larger genus- n cells is described in Section VII. Experimental results from simulations are collected in Section VIII, with final concluding remarks gathered in Section IX.

II. RELATED WORKS

Almost all state-of-the-art methods to solve the coverage path planning (CPP) problem [5] [7] first divide the target surface into cells then solve the CPP problem in each cell, so called cellular decomposition, which is further divided into two categories: exact cellular decomposition methods [13] and Morse-based cellular decomposition methods [6] [1].

For the optimal coverage task with a manipulator, the algorithms mainly focus on workspace metrics such as path length and time to completion. Atkar *et al.* [3] optimised the coverage path through choosing optimal starting points. Huang [10] reduced movement cost by remaining on straight paths as long as possible thus minimising the number of turns. In dealing with the optimal Non-revisiting Coverage Path Planning (NCP) problem, [2] considered the uniform coverage in automotive spray painting problem, where the simple back-and-force boustrophedon path was deformed in accordance to the curvature and topology of the surface. [8] proposed a 3D coverage path for agricultural robots minimising the skip/overlap areas between swaths.

¹A video illustrating the concepts hereby described can be found here:https://github.com/ZJUTongYang/RSS20/blob/master/supplementary_video.mp4

It is arguable however that for surface contact tasks in particular, the cost incurred in joint discontinuities significantly outweighs other metrics, moreover where undesirable transitions between position and force/torque control [4] [9] [14] [18] [19] become unavoidable.

We notice that [16] considered the pose optimisation of a mobile manipulator for coverage task, where a quality measurement was proposed to optimally place the manipulator in the workspace to aid coverage. The focus remained complementing robot placement and CPP; the actual generation of the coverage path simply reduced to use a randomised path planner, BiRRT [11] among a set of "guard points" chosen, with no specific consideration to joint-space continuity as elaborated in the present manuscript.

It is worthwhile noting that despite the apparent similarities in planning with mobile platforms, the optimal NCP problem with least discontinuities is inherent to the kinematics of manipulator mechanisms, and as such beyond the scope of bibliographic works from the mobile robotics community. Likewise, affinities to graph theory are also legit. Note however that the contact point, which can be safely regarded as a particle, is significantly smaller than the scale of the cellular decomposition drawn up for this problem. In seeking maximal joint-space continuity of the coverage path travelled by a particle as modelled by the NCP problem, infinitesimal elements must be considered in its most abstract form, and the existence of infinitely narrow passages also makes a significant difference in the resulting path solutions. Hence, it is not possible to revert back to classical graph theory since no area on the surface can be seen as a whole to form the "vertices", and the set of "edges" is actually the exact solution the NCP problem is seeking to solve for.

III. PROBLEM STATEMENT

Define the surface of an object by M . To simplify the description, let M be only the coverable part of the surface. The shape of other obstacles in the workspace and their relative poses in the workcell are assumed static and known. Given the kinematics of the non-redundant manipulator, we denote the joint-space by \mathcal{C} , and the set of all singular configurations by S . The set of all valid manipulator configurations is denoted by \mathcal{C} , where the validity of a configuration is evaluated by some given quality constraints denoted by $\{F_k\}_{k \in \mathbb{N}}$. Classic examples would be manipulability or the minimum distance from an obstacle. The optimal CPP problem is to find a joint-space path consisting of valid configurations whereby the manipulator EE covers the workspace non-repetitively and ensures the least number of discontinuities requiring lifting from the object's surface. The following settings define the scope formally:

- 1) A point contact between surface and EE is assumed.
- 2) Let $s \in S$ be a singular configuration, there exist a threshold $\varepsilon > 0$ such that

$$d(c, s) > \varepsilon, \forall c \in \mathcal{C}, \forall s \in S \quad (1)$$

where $d(\cdot, \cdot)$ is a metric in the joint-space. This enables us to judge the discontinuity of two configurations coming from discretised data. For example, given two configurations $c_1, c_2 \in \mathcal{C}$ corresponding to the EE covering two adjacent vertices of a triangular mesh, we say c_1 and c_2 are joint-space continuous only if

$$d(c_1, c_2) < \varepsilon \quad (2)$$

where $d(\cdot, \cdot)$ and ε are pre-determined.

- 3) $\{F_k\}_{k \in \mathbb{N}}$ is continuously defined in the joint-space, with thresholds satisfying strict inequalities. The k -th constraint can be expressed as

$$F_k(c) > \delta_k = \delta_k(c, F_1, \dots, \hat{F}_k, \dots, F_n), \forall c \in \mathcal{C} \quad (3)$$

where “ $\hat{\cdot}$ ” means excluding the term. δ_k can be a function of other metrics instead of a constant value, leading to wider applications. For example, let F_1 represent the manipulability [21] and F_2 represent the minimum distance between the manipulator and all obstacles, then an inequality such as

$$F_2(c) > \delta_2 = 0.01 + 0.05(1 - F_1(c))$$

could be imposed to indicate that when $F_1(c)$ is small, i.e. a “badly-conditioned” configuration, it should be farther from obstacles than would be desirable otherwise.

IV. FINITENESS OF CELLS

For a non-redundant manipulator, $\forall m \in M$ there exist a finite number of valid configurations to cover m . By following the constraints laid out in the problem statement, a topological graph will be generated. A necessary condition to solve it is thus guaranteeing the finiteness in the number of cells on this graph. For that, let us define a topological cell C_1 (where 1 represents its index) as a maximal set of continuous points where the valid configurations to cover them are pairwise continuous, i.e., $\forall m, m' \in C_1$, let the valid configurations to cover them be

$$P_m = \{c_{m1}, \dots, c_{mN}\} \subset \mathcal{C} \quad (4)$$

$$P_{m'} = \{c_{m'1}, \dots, c_{m'N'}\} \subset \mathcal{C} \quad (5)$$

then $N = N'$ and $\forall c_{mi} \in P_m, \exists c_{m'j} \in P_{m'}, c_{mi}$ and $c_{m'j}$ are joint-space continuous.

A topological edge E_1 (where 1 represents its index) is a maximal set of continuous points between C_i and C_j whereby

$$\begin{aligned} E_1 &= E_1(C_i, C_j) \\ &= \{m \in M | \forall (m \in) U_m, \exists p, p' \in U_m, p \in C_i, p' \in C_j\} \end{aligned} \quad (6)$$

Note that the intersecting points of topological edges

$$\{m | \forall (m \in) U_m, \exists p, p', p'' \in U_m, p \in C_i, p' \in C_j, p'' \in C_k\} \quad (7)$$

are distinct points, which is negligible when discussing the connectivity of the cells. The topological graph is the ordered cells and edges, $G = (\{C_i\}, \{E_j\})$.

To prove the finiteness of this graph, let us randomly choose a point $m \in M$ which can be covered by a set of valid configurations P_m defined by (4), then

$$F_k(c_{mi}) > \delta_k, \forall k, \forall i = 1, \dots, N \quad (8)$$

the strict inequalities (3) enable us to find valid open sets for each configuration in the joint-space:

$$\begin{aligned} &\exists (c_{mi} \in) U_{mi} \subset \mathcal{C}, \forall i = 1, \dots, N \\ \text{s.t. } &F_k(c) > \delta_k + \frac{1}{2}(F_k(c_{mi}) - \delta_k) > \delta_k, \forall k, \forall c \in U_{mi} \end{aligned} \quad (9)$$

since the kinematic function of the manipulator (FK) is continuous and $c_{mi} \in U_{mi}$,

$$m \in \text{FK}(U_{mi}) \subset M, \forall i = 1, \dots, N \quad (10)$$

so does the intersecting area of those images,

$$m \in A_m \triangleq \bigcap_{i=1}^N (\text{FK}(U_{mi})) \subset M, \forall i = 1, \dots, N \quad (11)$$

follow the definition of our topological cells, all points within the intersecting area belong to a same cell.

For $\forall m \in M$, the corresponding open set A_m exists, as such

$$\bigcup_{m \in M} A_m \supseteq M \quad (12)$$

hence the left term forms a infinite cover of M . The Heine-Borel Theorem [17] states that if a compact region can be covered by infinite many open regions, then one can find finite many of them that still fully cover this region. Since all closed sets in the Euclidean space are compact sets, so is the manipulator task space in which the boundaries are well-defined. Thus, we can find finite elements from $\{A_m\}_{m \in M}$ that also fully cover M . Recall that each A_m belongs to only one cell, hence the total number of cells in the graph must be finite.

V. SOLVING GRAPHS WITH SIMPLY-CONNECTED CELLS

In earlier work [20], the optimal NCPP problem with least discontinuities was also modelled as a topological cell graph, and the solution transformed into an optimal design strategy of a colour (configuration) scheme, as per the example illustrated by Fig 1. In proving the finiteness of simply-connected cells, the following claims were validated:

- 1) It is sufficient to consider cutting paths that start and end at the topological edge end-points.
- 2) It is unnecessary to consider cutting paths that stretch across edges.
- 3) Intersecting cutting paths can be discarded.
- 4) For a simply-connected cell with K topological edges delineating its boundary, a binary number of length K can uniquely specify the set of all admitted divisions.
- 5) To solve a simply-connected cell with K edges, the total number of different divisions is bound by

$$\Psi(K) = \Phi(K) \leq 2^K \quad (13)$$

where Ψ and Φ are both defined for later consistency. In the following sections, a generalisation to genus- n cells is derived.

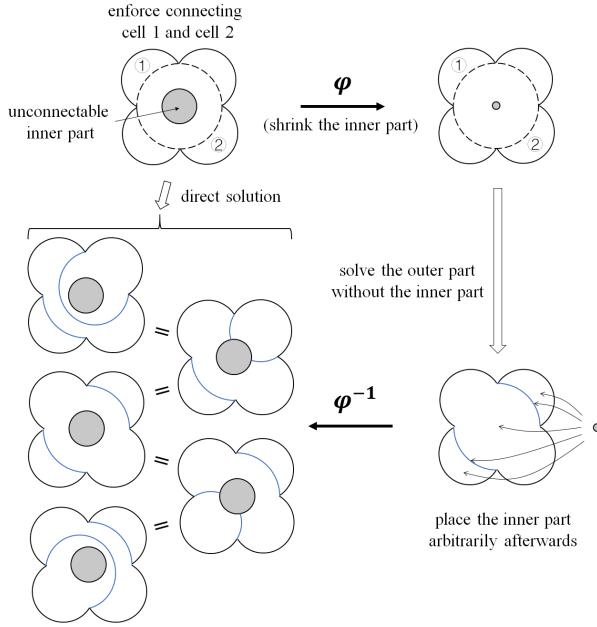


Fig. 3. Example showing that the unconnectable inner part (marked by the grey solid circle) is negligible when solving the outer part. ω and ω' are directly drawn as concentric circles so $\varphi(\omega') = \omega'$. In this simple example the direct solutions are straightforward, and they are equivalent to first solving the outer part without the inner part, and then arbitrarily replacing back the inner part.

VI. SOLUTION OF GENUS-ONE CELLS

A cutting path connecting the inner part and the outer part of a genus-one cell will transform the cell into a simply-connected cell, proven to be finitely solvable. In this section we consider two cases: keeping the genus-one structure or transforming the genus-one cell into simply-connected subcells. In the former case, we prove that the inner part and the outer part can be seen as two independent problems. While in the later case, by efficiently discarding equivalent cellular decompositions, the number of possible subdivisions is proven to be finite, and all optimal solutions thus finitely solvable. An upper-bound on the complexity of solving a genus-one cell is also derived.

For notation, a genus-one cell is denoted by Ω , with its inner boundary and outer boundary denoted by ω and ω' , respectively. The edges and cutting paths are denoted by α .

A. Independence of Inner and Outer Parts

The situation when inner part and the outer part of Ω are not connected arises when the inner part is a physical hole, the inner part can only be covered with a totally different colour from that of the outer part, or when all the edges in ω must be retained. In these cases, first we prove that the inner part of Ω is negligible when solving the outer part. To show this equivalence, let φ be a homeomorphic mapping from Ω to the standard unit disk D , with its boundaries mapped onto concentric circles,

$$\varphi : \Omega \rightarrow D, \omega' \mapsto S^1(1), \omega \mapsto S^1(\delta), \delta \rightarrow 0^+ \quad (14)$$

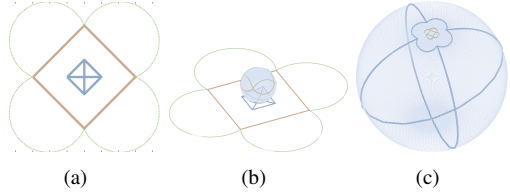


Fig. 4. (a) Topological graph with a genus-one cell enforced to be kept (the area between concentric squares). (b) A stereographic projection using a sphere lying within the inner boundary. (c) Let the radius of the sphere be small enough, then the inner part of graph and the outer part interchange near the north pole of the sphere.

then the inner part becomes an infinitesimal open neighbourhood of the origin. See Fig. 3 for illustration. Let a cutting path of D , $\varphi(\alpha)$, start and end at $\varphi(\omega')$, then it must be one of the following two cases:

$$\begin{aligned} & (0,0) \notin \varphi(\alpha) \\ & \Rightarrow \exists \varepsilon > 0, B(0, \varepsilon) \cap \varphi(\alpha) = \emptyset \\ & \Rightarrow \text{let } \delta < \varepsilon, \text{ then } \varphi(\omega) \cap \varphi(\alpha) = \emptyset \\ & \Rightarrow \omega \cap \alpha = \emptyset \end{aligned} \quad (15)$$

or

$$\begin{aligned} & (0,0) \in \varphi(\alpha) \\ & \Rightarrow \varphi(\omega) \cap \varphi(\alpha) \neq \emptyset, \forall \delta \\ & \Rightarrow \omega \cap \alpha \neq \emptyset \end{aligned} \quad (16)$$

All the different topological divisions described by (15) and (16) correspond to those listed in Fig. 3.

Next, we prove the inverse claim that the outer part of Ω is negligible when solving the inner part. Let a sphere with radius r stand within the inner part (anywhere is applicable but a place within the inner part will simplify the description), and ψ be the stereographic projection

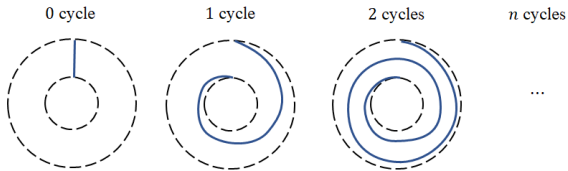
$$\begin{aligned} \psi : \mathbb{R}^2 & \rightarrow S^2 \setminus N \\ (x, y, 0) & \mapsto \left(\frac{4r^2 x}{x^2 + y^2 + 4r^2}, \frac{4r^2 y}{x^2 + y^2 + 4r^2}, \frac{2r(x^2 + y^2)}{x^2 + y^2 + 4r^2} \right) \end{aligned} \quad (17)$$

where N denotes the arctic point. See Fig. 4 for illustration. Since ψ is homeomorphic, the transformed graph on the sphere is equivalent to the original graph. ψ maps the outer part (including the uncoverable ambient space) to a neighbourhood of the arctic point (the ∞ point to the arctic point), and the inner part to a neighbourhood of the antarctic point. Let $r \rightarrow 0$, the roles of the inner part and the outer part interchange near the arctic point. Recalling the observation of the negligibility of the inner part, we finish the proof.

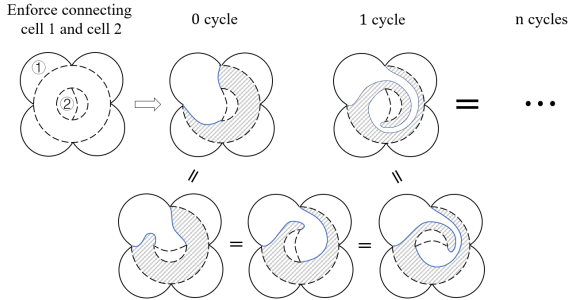
In summary, when the inner part and the outer part are not connected, they can be solved independently and their results can be merged directly.

B. Negligibility of Cyclic and Single Cutting Paths

Cutting paths connecting ω and ω' can be classified based on their number of cycles, as depicted by Fig. 5(a). However, Fig. 5(b) shows that all cyclic cutting paths have the same topological function as the acyclic one, thus can be safely



(a) Each acyclic cutting path corresponds to a family of cyclic cutting paths that go through different cycles.



(b) Continuous transformation between the 0-cycle division and 1-cycle division, with similar results for the n -cycles case.

Fig. 5. Examples of negligible cutting paths.

disregarded. Note however that unlike the case for other equivalences, the physical cellular decomposition using the cyclic cutting paths cannot be generated through continuously modifying the position of the acyclic ones. Here the equivalence means that only the acyclic situations require explicit consideration. Once an acyclic solution is optimal, all equivalent solutions using the cyclic cutting paths are all optimal and automatically considered.

Next, we observe that if there is only one cutting path that connects ω and ω' , then Ω is transformed into a single simply-connected sub-cell. However, this becomes a contradiction since both sides of the cutting paths are effectively the same cell, thus impossible to have different colors. It is therefore apparent that it is not the cutting path but the connected area what determines the division of Ω . More precisely, an area connecting the inner part and the outer part of Ω . This observation motivates us to directly consider the connectivities between cells. Based on the remarks in Section V, we only need to judge whether keeping or removing each edge. Let the indices of J edges in ω and K edges in ω' be (in cyclic order)

$$\omega = (\alpha_1, \dots, \alpha_J) \quad (18)$$

$$\omega' = (\alpha'_1, \dots, \alpha'_K). \quad (19)$$

Arbitrarily choosing some edges in ω and ω' to generate a connectivity, like

$$(\{\alpha_{i_1}, \dots, \alpha_{i_r}\}, \{\alpha'_{j_1}, \dots, \alpha'_{j_s}\}), 1 \leq r \leq J, 1 \leq s \leq K \quad (20)$$

where $\{\}$ means the order has no meaning, leads to valid divisions of the Ω . An example is shown in Fig. 6, where it is apparent that results are not unique. The finiteness of this approach is discussed next.

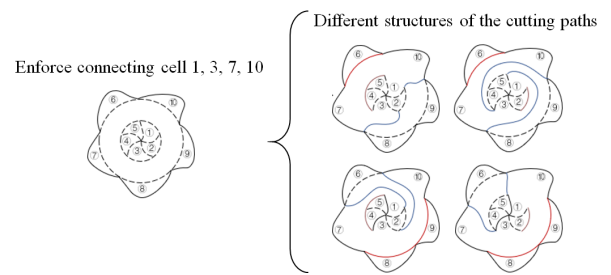


Fig. 6. In this example, cell 1, 3, 7 and 10 are enforced to be connected. We can see at the right side there are four different divisions having the same function.

C. Assignment of Cutting Paths Based on Connectivity

Extracting all combinations from (20) does not necessarily mean listing all different divisions. In Fig. 6, various divisions are created from the same connectivity. In order to address this issue, the whole division of Ω is regarded as a two-stage process, first transforming into simply-connected sub-cells and then undertaking further divisions in these sub-cells. We prove that in the first stage, only two cutting paths are required which connect ω and ω' .

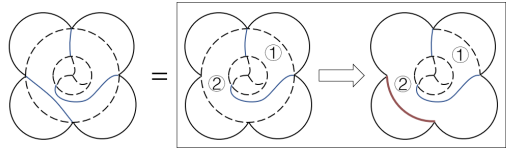
First, all cutting paths that do not connect ω and ω' do not appear in the first stage, because they can be seen as further divisions in the generated sub-cells. Refer to Fig. 7 for an illustration of this phenomenon. Then, let there be three cutting paths that connect ω and ω' , then Ω is divided into three simply-connected cells. However, the resulting topological structure is equivalent to Ω being firstly divided into two sub-cells, then another cutting path creating further divisions iteratively. Hence, there need to be at most two cutting paths in the first-stage.

In summary, let ω and ω' be defined by (18) and (19), during the first stage a continuous subset is identified in ω , and another one in ω' . The total number of different divisions is the number of different choices of these continuous subsets. To relieve the problem of the cyclic choices, we enforce the sub-cell 1 be the one containing α_1 . So all choices in ω are described by

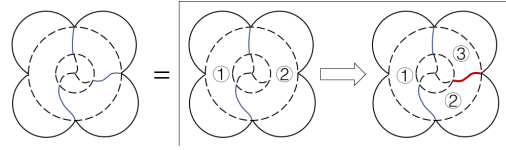
$$\left\{ \begin{array}{l} \{\alpha_1\} \\ \{\alpha_1, \alpha_2\}, \{\alpha_J, \alpha_1\} \\ \dots \\ \{\alpha_1, \dots, \alpha_{J-1}\}, \dots, \{\alpha_3, \dots, \alpha_J, \alpha_1\}. \end{array} \right. \quad (21)$$

Likewise, all choices in ω' are given by

$$\left\{ \begin{array}{l} \{\alpha'_1\}, \{\alpha'_2\}, \dots, \{\alpha'_K\} \\ \{\alpha'_1, \alpha'_2\}, \dots, \{\alpha'_K, \alpha'_1\} \\ \dots \\ \{\alpha'_1, \dots, \alpha'_{K-1}\}, \{\alpha'_K, \alpha'_1, \dots, \alpha'_{K-2}\}, \dots, \{\alpha'_2, \dots, \alpha'_K\} \end{array} \right. \quad (22)$$



(a) Illustration of cutting paths that start and end at the same boundary, which can be seen as further divisions (in sub-cell 2, shown in red).



(b) Example shows that the third (and later) cutting paths connecting ω and ω' can be seen as further divisions (in sub-cell 2, shown in red).

Fig. 7. Iterative process of cutting paths in stages.

D. Complexity Analysis

When ω and ω' are connected, there are r methods to choose r continuous edges in ω containing α_1 , i.e.,

$$\{\alpha_{J-r+1}, \dots, \alpha_J, \alpha_1\}, \dots, \{\alpha_1, \dots, \alpha_r\} \quad (23)$$

and K methods to choose s continuous edges in ω' . Summarising all possible r and s we get

$$\Psi(J, K) = \sum_{r=1}^{J-1} \sum_{s=1}^{K-1} rK\Phi(r+s)\Phi(J+K-r-s) \quad (24)$$

with Φ defined by (13). Moreover, from Section VI-A, the number of different divisions keeping a genus-one structure is

$$\Phi_0(J, K) = \Phi(J) + \Phi(K) = 2^J + 2^K \quad (25)$$

hence the total number of different divisions for a genus-one cell with J edges in the inner boundary and K edges in the outer boundary is given by

$$\Phi(J, K) = \Phi_0(J, K) + \Psi(J, K) \quad (26)$$

VII. SOLUTION OF LARGE GENUS CELLS

There are n inner boundaries in a genus- n cell. Taking the outer boundary into consideration, there are C_{n+1}^2 possible “starting- ending-point” pairs for the possible cutting paths, which are impractical to enumerate and deal with. Hence, a multi-stage iterative strategy is once again proposed to transform a genus- n cell into sub-cells with genus no more than $n - 1$.

A. Genus-Two Cell Case

Following a deduction process similar to the one in Section VI-A), the ensuing equivalence states arise:

- 1) The disconnected inner part can be safely discarded and the remaining becomes a genus-one cell which has been proved solvable. After solving both the genus-one cell and the unconnectable part independently, we can arbitrarily place the resulting division of the disconnected inner part in the result of the genus-one cell.

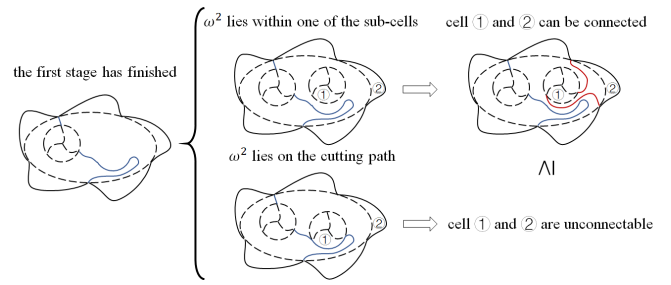


Fig. 8. Example showing that at each stage, cost-wise it is unnecessary to place the second inner part on the cutting paths created earlier (in blue).

- 2) When both inner parts are unconnectable, the genus-two cell can be seen as three simply-connected parts. And the solution comes from the arbitrary placements of the solution of the inner parts in the result of the outer part.

For a genus- n cell, if any of its inner part is disconnected, the genus- n problem becomes a genus- $(n - 1)$ problem which is proven solvable under induction. Hence, in this section the focus is on the case when all boundaries are forced to be connected.

Following the notation of a genus-one cell, a genus-two cell is denoted by Ω , with its outer boundary described by

$$\omega = (\alpha_1, \dots, \alpha_K) \quad (27)$$

and the inner boundaries given by

$$\omega^1 = (\alpha_1^1, \dots, \alpha_{J_1}^1) \quad (28)$$

$$\omega^2 = (\alpha_1^2, \dots, \alpha_{J_2}^2) \quad (29)$$

where α_* are the edges in each boundary listed in cyclic order.

Similar to the process illustrated in Section VI, we regard the whole division of Ω as a three-stage process. In the first stage, we consider the generation of the cutting paths connecting ω and ω^1 . As per the discussion in Section VI-C, at this point there are only two cutting paths, generating two sub-cells. In the second stage, we place ω^2 in each of the sub-cells. In either case, the sub-cell containing ω^2 becomes a genus-one cell. Then it can be solved through further division. After creating other two cutting paths, Ω is transformed into three simply-connected sub-cells. In the third stage, all other cutting paths are created.

B. Negligibility of Putting Inner Part on the Cutting Paths

A special case may first appear to arise when placing ω^2 within each sub-cell generated in the first stage intersecting the actual cutting path created (seen in blue in Fig. 8) Yet this is a case that requires no consideration given the equivalence shown in the same Figure. Since ω^2 is not assumed unconnectable, if a cutting path lies on the existing topological edges, it prevents further connections (such as the one shown in red in Fig. 8), leading to higher cost. Recalling the result from Section VI-C, there are only two cutting paths dividing Ω into two parts, so there are exactly two different places to put ω^2 , i.e., in either sub-cell created in the first stage.

C. Complexity Analysis of Solving Genus-2 Cells

When ω^1 and ω^2 are both disconnected, similar to (25), we have

$$\Phi_{00}(J_1, J_2, K) = 2^{J_1} + 2^{J_2} + 2^K \quad (30)$$

If ω and ω^1 are connected, but ω^2 is disconnected,

$$\Phi_{10}(J_1, J_2, K) = \Psi(J_1, K) + \Phi(J_2) \quad (31)$$

exchanging the role of ω^1 and ω^2 ,

$$\Phi_{01}(J_1, J_2, K) = \Psi(J_2, K) + \Phi(J_1) \quad (32)$$

When both ω^1 and ω^2 are connected, the complexity can be calculated by considering ω^2 being placed in different sub-cells separately. Using Ξ_1 for the situations that ω^2 is placed in sub-cell 1, and Ξ_2 for sub-cell 2 give rise to

$$\Xi_1(J_2; r_1, J_1, s, K) = \Psi(J_2, r_1 + s)\Phi(J_1 + K - r_1 - s) \quad (33)$$

$$\Xi_0(J_2; r_1, J_1, s, K) = \Phi(r_1 + s)\Psi(J_2, J_1 + K - r_1 - s) \quad (34)$$

Going through all possible r_1 and s , we have

$$\begin{aligned} \Psi(J_1, J_2, K) &= \sum_{r_1=1}^{J_1-1} \sum_{s=1}^{K-1} \\ &\quad r_1 K [\Xi_1(J_2; r_1, J_1, s, K) + \Xi_0(J_2; r_1, J_1, s, K)] \end{aligned} \quad (35)$$

Summarising (30), (31), (32) and (35), the final result is compounded by

$$\begin{aligned} \Phi(J_1, J_2, K) &= \Phi_{00}(J_1, J_2, K) + \Phi_{01}(J_1, J_2, K) \\ &\quad + \Phi_{10}(J_1, J_2, K) + \Psi(J_1, J_2, K) \end{aligned} \quad (36)$$

D. Genus- n Cell Case

Let Ω be a genus- n cell, with its outer boundary denoted by ω and inner boundaries denoted by $\omega^1, \dots, \omega^n$. The edges and their order in each boundary are given by (27) and

$$\omega^i = (\alpha_1^i, \dots, \alpha_{J_i}^i), \forall i = 1, \dots, n \quad (37)$$

Again, we assume that all ω^i must be connected, or else the disconnected inner parts can be safely discarded, then the genus- n problem becomes a lower-genus problem.

Similar to our discussion of the genus-two cell, the whole division of a genus- n cell can be seen as an $(n+1)$ -stage process. At each stage, ω^i is added to one of the sub-cells, transforming it into a genus-one sub-cell. Then, exactly two new cutting paths are required to transform this sub-cell again into two simply-connected sub-cells. After n -stages, Ω becomes an ensemble of simply-connected sub-cells. The process is illustrated by Fig. 9.

E. Complexity Analysis of Solving Genus- n Cells

The number of different divisions can be classified based on whether each inner part is connected. For a genus- n cell, define the subscript T_n as a binary string with length n , where the digit sum of T_n is $N(T_n)$. For example, $N(T_n) = 0$ represents the case that none of the inner boundaries are connected. In this case,

$$\Phi_{0\cdots 0}(J_1, \dots, J_n, K) = 2^{J_1} + \dots + 2^{J_n} + 2^K \quad (38)$$

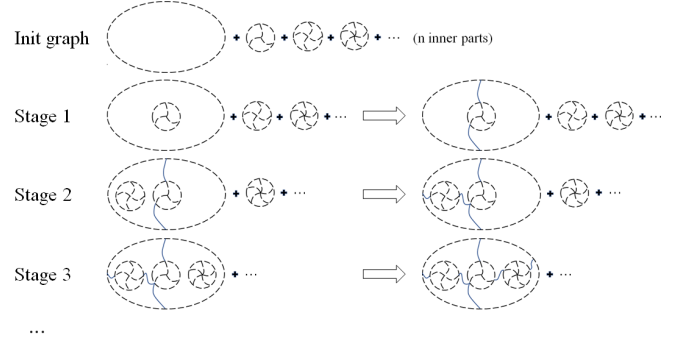


Fig. 9. Iterative transformation process of the genus- n case.

If $N(T_n) = 1$, e.g., ω and ω^1 are connected - and a genus- $(n-1)$ structure is kept after the whole division - the number of divisions are

$$\Phi_{10\cdots 0}(J_1, \dots, J_n, K) = \Psi(J_1, K) + 2^{J_2} + \dots + 2^{J_n} \quad (39)$$

There are $(C_n^1 - 1)$ terms with $N(T_n) = 1$, e.g., $\Phi_{010\cdots 0}$ to $\Phi_{0\cdots 01}$, that can be calculated through exchanging the indices. Similarly, an example for $N(T_n) = 2$ can be given by

$$\Phi_{110\cdots 0}(J_1, \dots, J_n, K) = \Psi(J_1, J_2, K) + 2^{J_3} + \dots + 2^{J_n} \quad (40)$$

and $(C_n^2 - 1)$ terms can be calculated through exchanging the indices,

$$\begin{aligned} &\dots \\ \Phi_{1\cdots 10}(J_1, \dots, J_n, K) &= \Psi(J_1, \dots, J_{n-1}, K) + 2^{J_n} \end{aligned} \quad (41)$$

with other $(C_n^{n-1} - 1)$ similar terms satisfying $N(T_n) = n-1$.

By induction, all the above mentioned terms can be calculated except for the one satisfying $N(T_n) = n$. After the first stage, we can choose which sub-cell each $\omega^i, i = 2, \dots, n$ will eventually lie in, and $\Xi_{T_{n-1}}$ are used to consider each situation, with the i -th binary digit in T_{n-1} representing that ω^i lies in sub-cell 1 or sub-cell 2. Let $B(T, i)$ be the value of the i -th digit in T ,

$$B(T, i) = \frac{T}{2^{n-i}} \bmod 2 \quad (42)$$

then

$$\begin{aligned} \Xi_{T_{n-1}}(J_2, \dots, J_n; r_1, J, s, K) \\ = \Psi(J_{i_2}, \dots, J_{i_p}, r_1 + s)\Psi(J_{i_{p+1}}, \dots, J_{i_n}, J + K - r_1 - s) \end{aligned} \quad (43)$$

where i_2, \dots, i_n are specified by

$$\begin{cases} B(T_{n-1}, i_j) = 1, & j = 2, \dots, P \\ B(T_{n-1}, i_j) = 0, & j = P+1, \dots, n. \end{cases} \quad (44)$$

It is easy to see that the order of J_{i_*} does not effect the result in (43). So

$$\begin{aligned} \Psi(J_1, \dots, J_n, K) &= \sum_{r_1=1}^{J_1-1} \sum_{s=1}^{K-1} \\ &\quad \left(r_1 K \sum_{T_{n-1}=0}^{2^{n-1}-1} \Xi_{T_{n-1}}(J_2, \dots, J_n; r_1, J, s, K) \right) \end{aligned} \quad (45)$$

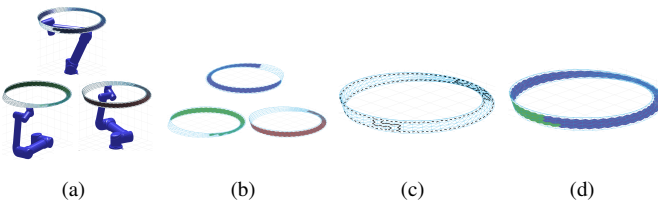


Fig. 10. Proposed NCPP applied to a Möbiüs strip (a) Examples of different configurations. (b) Coverable area of each the corresponding (colour) configuration. (c) Topological graph (d) One optimal solution requiring 1 lift-offs.

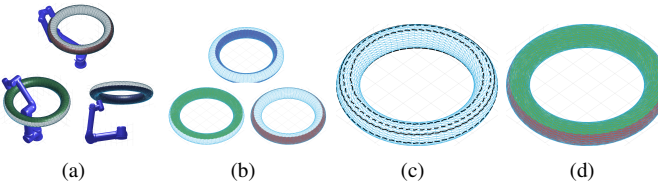


Fig. 11. Proposed NCPP applied to a closed surface ring(a) Examples of different configurations, where it becomes apparent that significant discontinuities will be inevitable without proper planning should the manipulator motion stretch in and out of the ring. (b) Continuous coverable area of three (colour) configurations, all of them being genus-one cells. (c) Topological graph generated. (d) One optimal solution, where only 1 lift-off is required.

Summarising the results from (38), (39), (40), (41), (45),

$$\Phi(J_1, \dots, J_n, K) = \sum_{T_n=0}^{2^n-2} \Phi_{T_n}(J_1, \dots, J_n, K) + \Psi(J_1, \dots, J_n, K) \quad (46)$$

VIII. EXPERIMENTAL RESULTS

Several representative simulation works have been implemented to validate the proposed algorithm on challenging arbitrarily-shaped objects. Fig. 10 presents the solution of polishing a Möbiüs strip, whose surface is non-orientable. The manipulator is required to maintain the EE normal to the surface for proper operation simulating a contact task such as polishing. This is rather challenging in this case since the strip is twisted, hence the orientation of the normal vector varies over the full 2π rads. However, the proposed algorithm is able to come up with an configuration mapping leading to an optimal solution where only 1 lift-off is required over the entire object.

Fig. 11 depicts the process of covering the surface of a “swimming” ring, another closed surface with no boundary. This is a particularly challenging case, it can be seen how the topological graph is formed by cells which are all multiply-connected, yet the proposed algorithm is able to come up with an effective solution with a single configuration discontinuity to the NCPP problem.

The examples in Fig. 2, Fig. 12 and Fig. 13 illustrate the solutions of covering a “hilly terrain” with varying degrees of desirable manipulability [21]. For a given configuration (colour) cell, the manipulability is explicitly depicted brighter for increasing manipulability for the given configuration. The threshold varies from a minium of 0.06 (Fig. 2) to at least 0.10

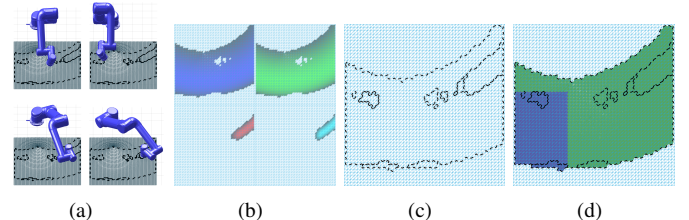


Fig. 12. (a) Examples of configurations belonging to different colours, where the threshold of manipulability at each point is set to > 0.1 . (b) Coverable area of the corresponding colours. We can see the wrist-flipped configurations can only cover reduced areas, and the configurations can no longer reach the area near the base of the manipulator (as compared with Fig. 2, where the minimum threshold is set to > 0.06). (c) Topological graph. (d) An optimal solution with 1 lift-off.

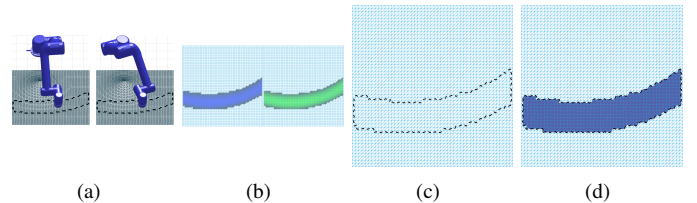


Fig. 13. Like Fig. 12, where the threshold of manipulability is set to > 0.16 .

(Fig. 12), up to at least 0.16, the maximum where a solution can be found for the object (in Fig. 13). As one would expect, a sharp reduction on the reachable area is observed as the manipulability tightens (mainly due to the limited mobility of the wrist-flipped configurations, shown in the bottom two configurations in Fig. 12(a)), causing large fluctuations in the structure of the resulting cells and topology graphs. When the threshold goes to 0.16, most of the kinematic-valid wrist-unflipped configurations are no longer valid, as depicted in Fig. 13.

IX. CONCLUSION

This paper has proposed a theoretical complete solution to the optimal non-revisiting coverage task problem of arbitrarily shaped objects with a non-redundant manipulator. Given topological graphs of surface cells corresponding to feasible and continuous manipulator configurations, the scheme ensures optimality with respect to the number of surface discontinuities, and is able to deal with non simply-connected space topologies, which arise for complex objects and as the number of task constraints limit the set of feasible configurations. In considering the generic solution to non simply-connected cells found in realistic environments, the proposed scheme effectively transforms the optimal CPP problem into an optimal colour designing problem of a topological configuration graph where a systematic solution for all genus cells is proposed. Through efficiently discarding equivalent and non-optimal cellular decompositions, the finiteness of divisions has been proven, and an upper bound in the number of divisions is calculated. Challenging simulation scenarios are provided to validate the proposed scheme.

REFERENCES

- [1] Ercan U. Acar, Howie Choset, Alfred A. Rizzi, Prasad N. Atkar, and Douglas Hull. Morse decompositions for coverage tasks. *The International Journal of Robotics Research*, 21(4):331–344, 2002. doi: 10.1177/027836402320556359.
- [2] P. Atkar, D. Conner, A. Greenfield, H. Choset, and A. Rizzi. Hierarchical segmentation of piecewise pseudoextruded surfaces for uniform coverage. *IEEE Transactions on Automation Science & Engineering*, 6(1):107–120.
- [3] Prasad Atkar, Howie Choset, and Alfred Rizzi. Towards optimal coverage of 2-dimensional surfaces embedded in \mathbb{R}^3 : choice of start curve. In *Proceedings of 2003 IEEE/RSJ International Conference on Intelligent Robots and Systems (IROS '03)*, volume 4, pages 3581 – 3587, October 2003.
- [4] Chien Chern Cheah, S Kawamura, and Suguru Arimoto. Brief stability of hybrid position and force control for robotic manipulator with kinematics and dynamics uncertainties. *Automatica*, 39(5):847–855, 2003.
- [5] Howie Choset. Coverage for robotics – a survey of recent results. *Annals of Mathematics and Artificial Intelligence*, 31(1):113–126, 2001.
- [6] Howie Choset, Ercan U Acar, A A Rizzi, and Jonathan Luntz. Exact cellular decompositions in terms of critical points of morse functions. 3:2270–2277, 2000.
- [7] Enric Galceran and Marc Carreras. A survey on coverage path planning for robotics. *Robotics and Autonomous Systems*, 61(12):1258–1276, 2013.
- [8] Ibrahim A Hameed, A La Courharbo, and Ottar L Osen. Side-to-side 3d coverage path planning approach for agricultural robots to minimize skip/overlap areas between swaths. *Robotics and Autonomous Systems*, 76:36–45, 2016.
- [9] D. Heck, Alessandro Saccon, N. Wouw, and Henk Nijmeijer. Switched position-force tracking control of a manipulator interacting with a stiff environment. *Proceedings of the American Control Conference*, 2015: 4832–4837, 07 2015. doi: 10.1109/ACC.2015.7172090.
- [10] W. H. Huang. Optimal line-sweep-based decompositions for coverage algorithms. In *Proceedings 2001 ICRA. IEEE International Conference on Robotics and Automation (Cat. No.01CH37164)*, volume 1, pages 27–32 vol.1, May 2001. doi: 10.1109/ROBOT.2001.932525.
- [11] Steven LaValle and James Kuffner. Randomized kinodynamic planning. *I. J. Robotic Res.*, 20:378–400, 01 2001.
- [12] Steven M. LaValle. *The Configuration Space*, page 105–152. Cambridge University Press, 2006. doi: 10.1017/CBO9780511546877.006.
- [13] V. J. Lumelsky, S. Mukhopadhyay, and K. Sun. Dynamic path planning in sensor-based terrain acquisition. *IEEE Transactions on Robotics and Automation*, 6(4):462–472, 1990.
- [14] Salehian Seyed Sina Mirrazavi and Billard Aude. A dynamical-system-based approach for controlling robotic manipulators during noncontact/contact transitions. *IEEE Robotics & Automation Letters*, 3(4):2738–2745.
- [15] G. Oriolo and C. Mongillo. Motion planning for mobile manipulators along given end-effector paths. In *Robotics and Automation, 2005. ICRA 2005. Proceedings of the 2005 IEEE International Conference on*, 2005.
- [16] Fabian Paus, Peter Kaiser, Nikolaus Vahrenkamp, and Tamim Asfour. A combined approach for robot placement and coverage path planning for mobile manipulation. In *2017 IEEE/RSJ International Conference on Intelligent Robots and Systems (IROS)*, 2017.
- [17] George F. Simmons. Introduction to topology and modern analysis. *The American Mathematical Monthly*, 71 (4), 1964.
- [18] J Ernesto Solanes, Luis Gracia, Pau Muñozbenavent, Alicia Esparza, Jaime Valls Miro, and Josep Tornero. Adaptive robust control and admittance control for contact-driven robotic surface conditioning. *Robotics and Computer-integrated Manufacturing*, 54:115–132, 2018.
- [19] J. Ernesto Solanes, Luis Gracia, Pau Muñoz-Benavent, Jaime Valls Miro, Carlos Perez-Vidal, and Josep Tornero. Robust hybrid position-force control for robotic surface polishing. *Journal of Manufacturing Science and Engineering*, 2018.
- [20] T. Yang, J. Valls Miro, Q. Lai, Y. Wang, and R. Xiong. Cellular decomposition for non-repetitive coverage task with minimum discontinuities. URL <https://arxiv.org/abs/2001.09577v1>.
- [21] Tsuneo Yoshikawa. Translational and rotational manipulability of robotic manipulators. *American Control Conference*, 27:228–233, 1990.